Available online at www.sciencedirect.com
SCIENCE DIRECT®

ELSEVIER

Polyhedron 23 (2004) 567–573

POLYHEDRON

www.elsevier.com/locate/poly

Syntheses and crystal structures of the potential tridentate ligand formed from condensation of ferrocenoylacetone and S-benzyldithiocarbazate and its bivalent metal complexes

Yao-Cheng Shi [a,*], Hua-Mei Yang [a], Hai-Bin Song [b], Chao-Guo Yan [a], Xiao-Ya Hu [a]

[a] *School of Chemistry and Chemical Engineering, Yangzhou University, Yangzhou 225002, PR China*
[b] *State Key Laboratory of Elemento-Organic Chemistry, Nankai University, Tianjin 300071, PR China*

Received 2 August 2003; accepted 14 October 2003

Abstract

A new potential tridentate ligand (**H_2L**) was synthesized from condensation of ferrocenoylacetone ($C_5H_5FeC_5H_4C(O)CH_2C(O)CH_3$) with S-benzyldithiocarbazate in refluxing benzene. Reaction of the ligand (**H_2L**) with a bivalent metal salt ($M(OAc)_2 \cdot xH_2O$, M = Cu, Ni, Mn, Hg, Zn; $SnCl_2 \cdot 2H_2O$) afforded the corresponding bivalent metal complexes M(**HL**)$_2$ (**I**, M = Cu; **II**, M = Ni; **III**, M = Mn; **IV**, M = Hg; **V**, M = Zn; **VI**, M = Sn). All the new compounds have been characterized by elemental analyses, ^{1}H NMR, IR and UV spectroscopies. A single-crystal X-ray analysis indicates that the ligand exists as a single iminone and not a tautomeric mixture of the iminone and enaminone. Crystallography of complex **VI** shows that the ligand acts as monoanionic tridentate coordinated to the tin atom via the carbonyl oxygen, deprotonated enamine nitrogen and thione sulfur atoms and the coordination geometry of the central metal is a distorted octahedron.

Keywords: Ferrocene; Dithiocarbazate; Ligand; Complex; Tin; Crystal structure

1. Introduction

N-substituted acid hydrazides are well-known to act as chelating agents [1–4]. Furthermore, these compounds and their metal complexes exhibit a broad spectrum of biological, bactericidal and fungicidal activities [5–7]. Since the discovery of ferrocene in 1951, it has played an important role in developing a knowledge of electronic structures of organometallic compounds and materials chemistry. A considerable number of ferrocene derivatives have been prepared directly or indirectly from ferrocene and their properties have been extensively studied. Among them, some have been reported to display biological activity and act as β-lactamase inhibitors [8,9]. In view of relatively few studies on reactions of 1,3-diketones and acylhydrazides, here we report the syntheses and crystal structures of the potential tridentate ligand [$C_5H_5FeC_5H_4C(O)CH_2C(CH_3){=}NNHCSSCH_2C_6H_5$] (**$H_2L$**) formed from condensation of ferrocenoylacetone and S-benzyldithiocarbazate and its bivalent metal complexes [10,11].

2. Experimental

2.1. Reagents and general procedures

All chemicals were of analytical grade and used without further purification. S-benzyldithiocarbazate and ferrocenoylacetone were synthesized according to the literature methods [12–14]. Progress of the reaction was monitored by TLC (silica gel H). The ^{1}H NMR spectra were determined with a Bruker Avance 500 spectrometer using TMS as an external standard in $CDCl_3$. IR spectra were recorded on a Perkin–Elmer 402 as KBr disks in the range of 400–4000 cm^{-1}. UV spectra were measured with a Shimadzu UV-240 spectrometer using a solution in DMF. Analyses for C, H

---

[*] Corresponding author. Tel/fax: +865147857939.
E-mail address: yzssyc@yzcn.net (Y.-C. Shi).

0277-5387/$ - see front matter © 2003 Elsevier Ltd. All rights reserved.
doi:10.1016/j.poly.2003.10.003

and N were performed on an Elementa Vario EL III microanalytical instrument. Melting points were measured on a Yanagimoto apparatus and uncorrected.

2.2. Synthesis of ligand

S-benzyldithiocarbazate (1.98 g, 10 mmol) was added to a solution of ferrocenoylacetone ($C_5H_5FeC_5H_4C(O)CH_2C(O)CH_3$) (2.7 g, 10 mmol) in 30 ml of benzene, the mixture was refluxed for 5 h and then evaporated to dryness and finally isolated by vacuum liquid chromatography (VLC), using a mixed solvent of CH_2Cl_2 and petroleum ether (v/v, 5:1) to afford the ligand. **H_2L** as orange red crystals, yield: 3.51 g (78%). M.p. 141–142 °C. *Anal.* Found: C, 58.48; H, 4.58; N, 5.89. Calc. for $C_{22}H_{22}FeN_2OS_2$: C, 58.66; H, 4.93; N, 6.22%. ^1H NMR (500 Mz, δ, in $CDCl_3$): iminone A isomer (shown in Scheme 1), 2.18 (s, CH_3), 3.73 (s, SCH_2), 3.94 (s, CH_2), 4.23 (s, C_5H_5), 4.55, 4.82 (s, s, $^3H/^4H$ and $^2H/^5H$ of C_5H_4 ring), 7.22–7.41 (m, C_6H_5), 6.54 (s, br, NH); enaminone B isomer (shown in Scheme 1), 2.07 (s, CH_3), 3.54, 3.58, 3.83, 3.86 (q, $^2J_{HH} = 18.6$ Hz, SCH_2), 4.21 (s, C_5H_5), 4.68, 4.78 (s, s, $^3H/^4H$ and $^2H/^5H$ of C_5H_4 ring), 5.73 (s, CH), 7.22–7.41 (m, C_6H_5), 9.82 (s, $NHCS_2$), 11.67 ppm (s, NH). IR (KBr disk): ν(NH) 3431(w, br), ν(C=O) 1665 (vs), ν(C=N) 1637 (m), ν (C=S) 1068 (vs), ν(C–S) 1035 (m), ν(N–N) 984 (m) cm^{-1}. UV (nm, in DMF): λ_{max} ($\varepsilon \times 10^4$, in $dm^3\ mol^{-1}\ cm^{-1}$) 405 (1.8) (K-band), 553 (0.053) (R-band). Single crystals of the ligand for X-ray determination were obtained by slow evaporation of its solution in dichloromethane and petroleum ether.

2.3. Syntheses of complexes

A solution of an appropriate metal acetate or $SnCl_2 \cdot 2H_2O$ (0.5 mmol) in 5 ml of absolute ethanol was added dropwise to a stirred solution of the ligand (**H_2L**) (0.45 g, 1 mmol) in 20 ml of absolute ethanol. The mixture was stirred for 6 h at room temperature and then filtered to afford the crude product. The resulting solid recrystallized from dichloromethane and petroleum ether gave the corresponding complex (**I** to **VI**).

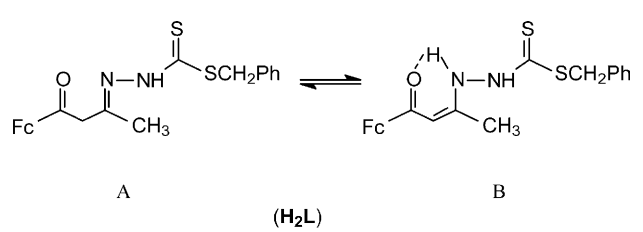

Scheme 1. Synthesis of ligand.

Complex **I** as a black solid, yield: 0.847 g (88%). M.p. 131–132 °C. *Anal.* Found: C, 54.54; H, 3.95; N, 5.42. Calc. for $C_{44}H_{42}Fe_2N_4O_2S_4Cu$: C, 54.92; H, 4.40; N, 5.82%. IR (KBr disk): ν(NH) 3435 (w, br), ν(C=O) 1664 (vs), ν(C=C) 1614 (m), ν(C=S) 1070(s), ν(C–S) 1019 (s), ν(N–N) 951 (m) cm^{-1}. UV (nm, in DMF): λ_{max} ($\varepsilon\times 10^4$, in $dm^3\ mol^{-1}\ cm^{-1}$) 265 (3.4) (B-band), 404 (4.5) (K-band).

Complex **II** as a dark red solid, yield: 0.536 g (56%). M.p. 158–158.5 °C. *Anal.* Found: C, 55.48; H, 4.08; N, 5.58. Calc. for $C_{44}H_{42}Fe_2N_4O_2S_4Ni$: C, 55.19; H, 4.42; N, 5.83%. ^1H NMR (500 Mz, δ, in $CDCl_3$): 1.83 (s, 6H, $2CH_3$), 4.37 (s, 4H, $2SCH_2$), 4.13 (s, 10H, $2C_5H_5$), 4.19–4.30, 4.63–4.69 (d, d, 4H, 4H, $^3H/^4H$ and $^2H/^5H$ of two C_5H_4 rings), 5.28 (s, 2H, 2CH), 7.22–7.40 (m, 10H, $2C_6H_5$), 8.28 ppm (s, 2H, 2NH). IR (KBr disk): ν(NH) 3434 (m), ν(C=O) 1663 (vs), ν(C=C) 1534 (m), ν(C=S) 1068 (s), ν(C–S) 1028 (m), ν(N–N) 966 (s) cm^{-1}. UV (nm, in DMF): λ_{max} ($\varepsilon \times 10^4$, in $dm^3\ mol^{-1}\ cm^{-1}$) 398 (2.0) (K-band), 624 (0.047) (R-band).

Complex **III** as a black purple solid, yield: 0.801 g (84%). M.p. 192–193 °C. *Anal.* Found: C, 54.90; H, 3.97; N, 5.50. Calc. for $C_{44}H_{42}Fe_2N_4O_2S_4Mn$: C, 55.41; H, 4.41; N, 5.87%. IR (KBr disk): ν(NH) 3427 (w, br), ν(C=O) 1529 (vs), ν(C=C) 1519 (vs), ν(C=S) 1062 (m), ν(C–S) 1020 (m), ν(N–N) 965 (m) cm^{-1}. UV (nm, in DMF): λ_{max} ($\varepsilon \times 10^4$, in $dm^3\ mol^{-1}\ cm^{-1}$) 387 (1.64) (K-band), 507 (0.052) (R-band).

Complex **IV** as a brown yellow solid, yield: 0.858 g (78%). M.p. 137 °C (dec.). *Anal.* Found: C, 47.77; H, 3.57; N, 4.77. Calc. for $C_{44}H_{42}Fe_2N_4O_2S_4Hg$: C, 48.05; H, 3.85; N, 5.10%. IR (KBr disk): ν(NH) 3434 (w), ν(C=O) 1666 (vs), ν(C=C) 1614 (m), ν(C=S) 1070 (m), ν(C–S) 1026 (m), ν(N–N) 944 (s) cm^{-1}. UV (nm, in DMF): λ_{max} ($\varepsilon \times 10^4$, in $dm^3\ mol^{-1}\ cm^{-1}$) 328 (1.74), 360 (1.72) (K-band).

Complex **V** as an orange yellow solid, yield: 0.868 g (90%). M.p. 192 °C (dec.). *Anal.* Found: C, 54.80; H, 4.09; N, 5.54. Calc. for $C_{44}H_{42}Fe_2N_4O_2S_4Zn$: C, 54.81; H, 4.39; N, 5.81%. IR (KBr disk): ν(NH) 3434 (w), ν(C=O) 1666 (vs), ν(C=C) 1622 (m), ν(C=S) 1071 (m), ν(C–S) 1024 (m), ν(N–N) 951 (m) cm^{-1}. UV (nm, in DMF): λ_{max} ($\varepsilon \times 10^4$, in $dm^3\ mol^{-1}\ cm^{-1}$) 265 (4.79), 277 (2.43) (B-band), 404 (3.74) (K-band).

Complex **VI** as an orange solid, yield: 0.916 g (90%). M.p. 238–239 °C. *Anal.* Found: C, 51.72; H, 4.22; N, 5.41. Calc. for $C_{44}H_{42}Fe_2N_4O_2S_4Sn$: C, 51.94; H, 4.16; N, 5.51%. ^1H NMR (500 Mz, δ, in $CDCl_3$): 2.45 (s, 6H, $2CH_3$), 4.31, 4.34, 4.53. 4.56 (q, 4H, $^2J_{HH} = 13.5$ Hz, $2SCH_2$), 4.21 (s, 10H, $2C_5H_5$), 4.37–4.39, 4.62–4.64 (d, d, 4H, 4H, $^3H/^4H$ and $^2H/^5H$ of two C_5H_4 rings), 5.39 (s, 2H, 2CH), 7.31–7.43 (2m, 10H, $2C_6H_5$), 7.28 ppm (s, 2H, 2NH). IR (KBr disk): ν(NH) 3439(w, br), ν(C=O) 1550 (s), ν(C=C) 1515 (vs), ν(C=S) 1051 (m), ν(C–S) 1018 (m), ν(N–N) 966 (m) cm^{-1}. UV (nm, in DMF): λ_{max} ($\varepsilon \times 10^4$, in $dm^3\ mol^{-1}\ cm^{-1}$) 400 (1.90) (K-band).

Table 1
Crystallographic data for ligand and complex **VI**

Formula	$C_{22}H_{22}FeN_2OS_2$	$C_{44}H_{42}Fe_2N_4O_2S_4Sn$
Formula weight	450.39	1017.45
Crystal size (mm)	$0.30 \times 0.25 \times 0.20$	$0.16 \times 0.14 \times 0.08$
Crystal system	triclinic	monoclinic
Space group	$P\bar{1}$	$P2_1/n$
Unit cell dimensions		
a (Å)	7.993(3)	16.452(7)
b (Å)	10.503(4)	10.819(5)
c (Å)	13.770(5)	23.932(10)
α (°)	108.573(6)	90.00
β (°)	90.576(6)	101.065(8)
γ (°)	102.356(6)	90.00
V (Å^3)	1066.6(6)	4180(3)
Z	2	4
D_c (g cm^{-1})	1.402	1.617
F (0 0 0)	468	2064
T (K)	293(2)	293(2)
μ(Mo Kα) (mm^{-1})	0.917	1.521
Scan mode	ϕ and ω scans	ϕ and ω scans
θ Range (°)	1.57–26.44	1.39–26.44
Limiting indices	$-9 \leqslant h \leqslant 8$, $-9 \leqslant k \leqslant 13$, $-17 \leqslant l \leqslant 16$	$-20 \leqslant h \leqslant 20$, $-13 \leqslant k \leqslant 13$, $-15 \leqslant l \leqslant 29$
Reflections collected	6149	19,253
Independent reflections	4318	8582
Number of parameters refined	279	516
Absorption correction	multi-scan	multi-scan
Final R indices [$I > 2.0\sigma(I)$]	$R = 0.0496$, $Rw = 0.1074$	$R = 0.0562$, $Rw = 0.1057$
R indices (all data)	$R = 0.0923$, $Rw = 0.1346$	$R = 0.1452$, $Rw = 0.1399$
Goodness-of-fitF	1.011	0.990
Largest peak and hole (e Å^{-3})	0.445 and −0.291	0.830 and −0.691

Single crystals of complex **VI** for X-ray determination were obtained by slow evaporation of its solution in dichloromethane and petroleum ether.

2.4. Crystal structure determination

For each of compounds (**H$_2$L** and **VI**), a selected single crystal was mounted on a Bruker SMART 1000 CCD diffractometer using graphite-monochromated Mo Kα radiation ($\lambda = 0.71073$ Å) at 293 K. Data collection and reduction were performed using the SMART and SAINT software [15]. An empirical absorption correction was applied using the SADABS program [16]. The structures were solved by direct methods and refined by full-matrix least-squares methods, based on F^2 with anisotropic thermal parameters for all non-hydrogen

Table 2
Selected bond distances (Å) and angles (°) for ligand

Bond distances			
Fe(1)–C(1)	2.027(3)	N(1)–C(13)	1.271(5)
Fe(1)–C(2)	2.047(4)	N(2)–C(14)	1.335(4)
Fe(1)–C(3)	2.056(4)	N(1)–N(2)	1.395(4)
Fe(1)–C(4)	2.047(4)	O(1)–C(11)	1.221(4)
Fe(1)–C(5)	2.033(4)	C(1)–C(11)	1.472(5)
Fe(1)–C(6)	2.044(4)	C(11)–C(12)	1.515(5)
Fe(1)–C(7)	2.029(5)	C(12)–C(13)	1.508(5)
Fe(1)–C(8)	2.041(5)	S(1)–C(14)	1.749(4)
Fe(1)–C(9)	2.051(4)	S(1)–C(15)	1.820(4)
Fe(1)–C(10)	2.044(4)	S(2)–C(14)	1.667(4)
Bond angles			
C(1)–C(11)–C(12)	116.8(3)	N(1)–C(13)–C(22)	126.9(3)
O(1)–C(11)–C(1)	121.4(3)	N(2)–C(14)–S(1)	113.9(2)
O(1)–C(11)–C(12)	121.8(3)	N(2)–C(14)–S(2)	121.4(3)
C(11)–C(12)–C(13)	112.9(3)	S(2)–C(14)–S(1)	124.7(2)
C(12)–C(13)–C(22)	117.5(3)	C(13)–N(1)–N(2)	117.4(3)
N(1)–C(13)–C(12)	115.6(3)	C(14)–N(2)–N(1)	119.4(3)

Table 3
Selected bond distances (Å) and angles (°) for complex **VI**

Bond distances			
Fe(1)–C(1)	2.010(7)	Fe(2)ndash;C(23)	2.026(7)
Fe(1)–C(2)	2.024(7)	Fe(2)–C(24)	2.016(8)
Fe(1)–C(3)	2.027(7)	Fe(2)–C(25)	2.045(8)
Fe(1)–C(4)	2.052(8)	Fe(2)–C(26)	2.025(8)
Fe(1)–C(5)	2.022(8)	Fe(2)–C(27)	2.019(7)
Fe(1)–C(6)	2.022(8)	Fe(2)–C(28)	2.012(9)
Fe(1)–C(7)	2.021(10)	Fe(2)–C(29)	2.054(9)
Fe(1)–C(8)	2.023(8)	Fe(2)–C(30)	2.059(9)
Fe(1)–C(9)	2.027(8)	Fe(2)–C(31)	2.032(9)
Fe(1)–C(10)	2.022(9)	Fe(2)–C(32)	1.989(9)
Sn(1)–O(1)	2.069(5))	Sn(1)–O(2)	2.061(5)
Sn(1)–N(1)	2.141(6)	Sn(1)–N(3)	2.137(6)
Sn(1)–S(1)	2.481(2)	Sn(2)–S(3)	2.487(2)
N(1)–C(13)	1.348(8)	N(3)–C(35)	1.333(9)
N(2)–C(15)	1.280(8)	N(4)–C(37)	1.262(9)
N(1)–N(2)	1.376(8)	N(3)–N(4)	1.382(8)
O(1)–C(11)	1.310(8)	O(2)–C(33)	1.311(8)
C(11)–C(12)	1.379(10)	C(33)–C(34)	1.371(9)
C(12)–C(13)	1.379(9)	C(34)–C(35)	1.407(10)
C(13)–C(14)	1.496(10)	C(35)–C(36)	1.502(9)
S(1)–C(15)	1.736(7)	S(3)–C(37)	1.745(8)
S(2)–C(15)	1.752(7)	S(4)–C(37)	1.744(8)
S(2)–C(16)	1.816(8)	S(4)–C(38)	1.801(8)
Bond angles			
N(1)–Sn(1)–N(3)	172.5(2)	Sn(1)–N(1)–N(2)	118.3(4)
O(1)–Sn(1)–O(2)	86.6(2)	S(1)–Sn(1)–S(3)	97.06(8)
O(1)–Sn(1)–N(1)	85.8(2)	S(1)–Sn(1)–N(1)	80.81(17)
O(1)–Sn(1)–N(3)	92.6(2)	S(1)–Sn(1)–N(3)	100.50(16)
O(1)–Sn(1)–S(1)	166.58(14)	S(1)–Sn(1)–O(2)	91.44(15)
O(2)–Sn(1)–N(1)	86.9(2)	S(3)–Sn(1)–N(1)	106.88(16)
O(2)–Sn(1)–N(3)	85.7(2)	S(3)–Sn(1)–N(3)	80.41(17)
O(2)–Sn(1)–S(3)	164.80(15)	S(3)–Sn(1)–O(1)	87.98(15)

atoms and hydrogen atoms were included in the model at their calculated positions and refined isotropically using the SHELXTL program package [17]. Crystal structure data and refinement details for both compounds are summarized in Table 1. Selected bond distances and angles are given in Tables 2 (**H_2L**) and 3 (**VI**).

3. Results and discussion

3.1. *Syntheses of ligand and its complexes*

Syntheses of ligand and its complexes are shown in Schemes 1 and 2. Reaction of ferrocenoylacetone ($C_5H_5FeC_5H_4C(O)CH_2C(O)CH_3$) and S-benzyldithiocarbazate in refluxing benzene via removal of water affords a new ligand (**H_2L**) as orange-red crystals. The ligand (**H_2L**) reacts with bivalent metal ions forming neutral complexes M(**HL**)$_2$ (**I,** M = Cu; **II,** M = Ni; **III,** M = Mn; **IV,** M = Hg; **V,** M = Zn; **VI,** M = Sn). TLC analysis of **H_2L** shows, that it exists as an equilibrium mixture of two isomers (major orange–red and minor brown spots) in solution. However, it can crystallize in an orange–red isomer. All complexes listed in Section 2 are soluble in polar organic solvents such as DMF, THF and dichloromethane and insoluble in non-polar organic solvents such as benzene, toluene and petroleum ether.

$$2\mathbf{H_2L} + \mathrm{M(OAc)_2} \xrightarrow{\text{Ethanol}} (\mathbf{HL})_2\mathrm{M} + 2\mathbf{H}\mathrm{OAc}$$

(M = Cu,Ni,Mn,Hg,Zn)

$$2\mathbf{H_2L} + \mathrm{SnCl_2} \xrightarrow{\text{Ethanol}} (\mathbf{HL})_2\mathrm{Sn} + 2\mathbf{H}\mathrm{Cl}$$

Scheme 2. Syntheses of complexes **I**–**VI**.

3.2. *^1H NMR Spectra*

The ^1H NMR spectral data of ligand (**H_2L**) and complexes **II** and **VI** are listed in Section 2. Although **H_2L** contains the thioamide $NHCS_2$ functional group, in principle, it can exhibit thione–thiol tautomerism. However, its ^1H NMR spectrum does not display any signal at approximately 4.00 ppm due to the H–S proton, indicating even in solution it exists as the thione tautomers (iminone A and enaminone B isomers) as shown in Scheme 1 [12], which is in agreement with the above TLC analysis of $\mathbf{H_2L}$. Two methyl groups of tautomers A and B exhibit two well-resolved singlets at δ 2.18 and 2.07 ppm. According to relative intensities of both singlets, two tautomers A and B exist in a 3:2 ratio in solution at room temperature. For tautomer A, the protons of SCH_2 and $COCH_2C$ moieties display two singlets at δ 3.73 and 3.94 ppm. The substituted cyclopentadienyl ring shows two singlets at δ 4.55 and 4.82 ppm which are due to protons of 3, 4- and 2, 5-positions, whereas a singlet at δ 4.23 ppm is due to protons on the unsubstituted cyclopentadienyl ring. The NH absorption appears at δ 6.54 ppm as a broad peak [11,19]. For tautomer B, the protons of $COCH{=}C$ moiety displays a singlet at δ 5.73 ppm while the protons of SCH_2 moiety exhibits a typical doublet–doublet quartet ($^2J_{HH} = 18.55$ Hz) [14,18]. The substituted cyclopentadienyl ring shows two singlets at δ 4.68 and 4.78 ppm which are due to protons of 3, 4- and 2, 5-positions, whereas a singlet at δ 4.21 ppm is due to protons on the unsubstituted cyclopentadienyl ring. The $NHCS_2$ (thioamide) and HN (enamine) absorptions appear at δ 9.82 and 11.67 ppm, respectively [14,19]. For both tautomers, benzene rings show three slightly-resolved multiplets at δ 7.22–7.41 ppm.

The ^{1}H NMR spectral data of complexes **II** and **VI** are characterized by the absence of the δ 3.94 ppm signal of $COCH_2C$ in the tautomer A or the δ 11.67 ppm signal of HN (enamine) in the tautomer B and the appearance of the methine (CH) at δ 5.28 and 5.39 ppm in complexes **II** and **VI** [14]. Therefore, the above evidence indicates that the ligand is deprotonated and bonded to the metal ion, which is also supported by the crystal structure of complex **VI** as described below. In addition, all the signals of protons in complex **II** display high-field shifts compared with those in the tautomer B, which may be due to the increase of electron density resulting from deprotonation and nickel-to-ligand feedback after forming the planar–square complex [2,14].

3.3. Crystal structures of ligand and complex VI

3.3.1. Crystal structure of ligand

The crystal structure of the ligand together with the atomic numbering scheme is shown in Fig. 1. The O(1)–C(11) (1.221(4) Å) and N(1)–C(13) (1.271(5) Å) bond distances indicate that these correspond to typical double bonds [20,21], so the ligand in the solid state exists in the form of the tautomeric iminone A. The N(1)–N(2) bond distance is 1.395(4) Å, which is slightly shorter than the single bond distance of 1.411(7) Å [11,21]. The C–S bond distances are 1.749(4) (S(1)–C(14)) and 1.820(4) Å (S(1)–C(15)). Of the two distances, one is close to the C–S distance of 1.81 Å, while the other shows an intermediate value between the single and double bond distances, indicating partial double bond character. The S(2)–C(14) distance (1.667(4) Å) is close to the C=S distance of 1.69 Å, suggesting that this is a double bond. Therefore, the above data indicate, that the bonding mode in the $NNCS_2CH_2Ph$ moiety is very similar to that in the S-benzyldithiocarbazate [22]. The average distance of iron to carbon in the ferrocenyl group is 2.042(4) Å and very close to 2.045 Å in ferrocene [23]. The mean C–C distances in the cyclopentadienyl rings with and without the side-chain are 1.422(5) and 1.403(7) Å and also close to 1.41 Å in ferrocene [23]. The distances of N(1)···S(1) (2.756(3) Å) and S(1)···S(2) (3.027 Å) fall in the range of the sum of van der waals radii of the corresponding two atoms (3.35 and 3.6 Å), which indicates that there is a weak interaction between the two atoms. Similarly, the distances of S(2)···H(2A) and S(2)···H(22A) show the existence of N(2)–H(2A)···S(2) and C(22)–H(22A)···S(2) intramolecular hydrogen bondings, whereas the O(1)···H(4) distance displays an O(1)···H(4)–C(4) intermolecular hydrogen bonding [24].

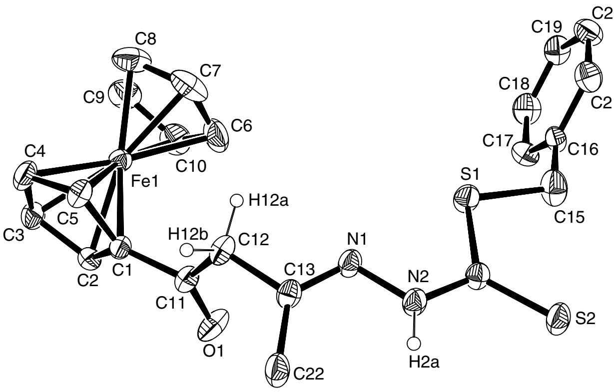

Fig. 1. Crystal structure of ligand.

3.3.2. Crystal structure of complex VI

The crystal structure of the new tin complex **VI** together with the atomic numbering scheme is shown in Fig. 2. The complex consists of two monoanionic tridentate ligands ($\mathbf{HL^-}$), each of which coordinates to the Sn(II) ion via carbonyl oxygen, deprotonation enamine

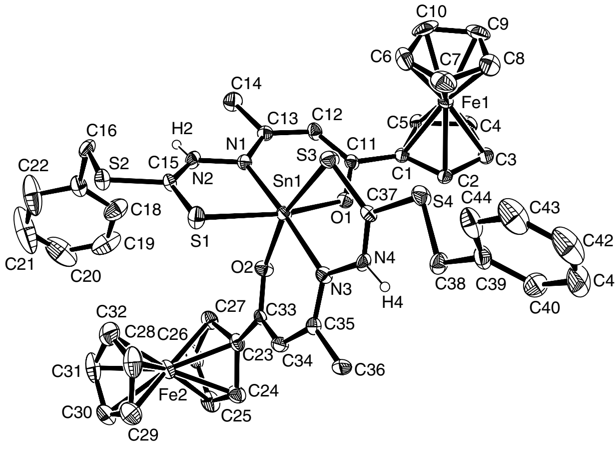

Fig. 2. Crystal structure of complex **VI**.

nitrogen and thione sulfur (ONS donor set), viz., through the deprotonated tautomer B. The coordination geometry of the central metal ion is a distorted octahedron, the bond angle of N(1)–Sn–N(3) being 172.5(2)°. The Sn–S, Sn–O and Sn–N bond distances are larger than values reported for a related complex (2.458(3), 2.396(3) and 2.187(4) Å) [25].

A comparison of the bond distances within the coordinated **HL**$^-$ ligands shows extensive delocalization to be present. The N–N bond at mean 1.379(8) Å, which is singnificantly shorter than the single bond distance of 1.411(7) Å, is observed to have some double bond character [12,21]. More double bond character is present in the C–N bond of the $HNCS_2$ moiety as judged from its bond distance of mean 1.271(8) Å. This very clearly indicates a pronounced lone pair delocalization between carbon and nitrogen, namely the p–π conjugation. More interestingly, formal C=S and C–S bonds in the $HNCS_2$ moiety also display marked electron delocalization [12,21]. The C–N bond distances (1.348(8) and 1.333(9) Å) in the $CH{=}C(CH_3)N$ moiety are close to the value of the C–N single bond (1.335(4) Å) of the $HNCS_2$ moiety in the free ligand while the C=O bonds are longer than the corresponding bond in the free ligand [20,21]. In addition, delocalization evidence is further supported by the fact that the hybridized states of C (attached to N and O atoms) and N atoms are all sp^2. Although that the protons of thioamide $NHCS_2$ functional groups are not removed on complexation are unusual, similar cases also appear in two metal complexes of thiosemicarbazone and dithiocarbazate ligands [26,27]. The average distance of iron to carbon (2.026(7) Å) and mean C–C distances with and without side-chains (1.42(1) and 1.39(1) Å) in the ferrocenyl groups are all shorter than those in the free ligand [2]. The distance of N(2)···H(16B) (2.43 Å) indicates that there is the C(16)–H(16B)···N(2) intramolecular hydrogen bonding in complex **VI**. It is more noted that although it contains the NH group no intermolecular hydrogen bonding about the NH group in complex **VI** is observed because of the steric hindrance from the methyl and benzyl groups. However, the S(2)···H(36A) distance (2.85 Å) may display a weak S(2)···H(36A)–C(36) intermolecular hydrogen bonding [24].

3.4. IR spectra

The important IR absorptions of the ligand (**H$_2$L**) and its complexes are given in Section 2. The ligand shows bands at ca. 3169, 1665, 1637, 1068, 1035 and 983 cm^{-1} which are assignable to ν(NH), ν(C=O), ν(C=N), ν(C=S), ν(C–S) and ν(N–N), respectively. The ν(C=N) band disappears and new bands at 1513–1622 and 1220–1287 cm^{-1}, which can be assigned to ν(C=C) and ν(C–N), are observed. For complexes **I, II, IV** and **V,** the ν(C=O) band remains nearly unchanged, whereas for complexes **III** and **VI** the corresponding band shows a significant red-shift compared with the free ligand. These facts indicate that the ligand possesses two bonding modes: as an NS bidentate bonded to Cu, Ni, Hg and Zn ions and as an ONS tridentate coordinated to Mn and Sn ions (N, deprotonation enamine nitrogen and S, thione sulfur) [12,14]. The ONS bonding mode has confirmed by the above crystal structure of complex **VI,** however efforts to grow single crystals of complex **I, II, IV** or **V** in order to further support the NS bonding mode were unsuccessful.

3.5. UV spectra

The UV spectral data of the ligand (**H$_2$L**) and its complexes are listed in Section 2. The UV spectrum of the ligand shows two absorptions at 405 and 553 nm, which are attributable to the K-band of the skelton [C(O)CH=C(CH$_3$)N] and the R-band (n → π* transition) [12,18,21]. For complex **I,** the shortest wavelength absorption which is assigned as the B-band of the benzene and cyclopentadienyl rings. However, complex **V** exhibits two B-bands of the benzene and cyclopentadienyl rings. Interestingly, the K-bands in all complexes show hypsochromic shifts compared with that of the free ligand [2].

4. Summary and conclusions

Reaction of ferrocenoylacetone and S-benzyldithiocarbazate yields a new ligand (**H$_2$L**). The ligand exists as a single iminone in the solid state while as a tautomeric mixture of the iminone and enaminone (3:2) in solution.

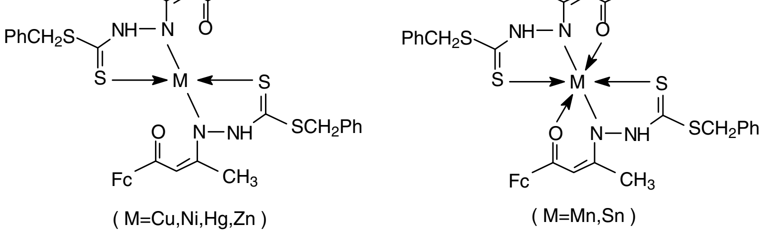

Fig. 3. Proposed structures of complexes.

Upon coordinating to the bivalent metal ion, the ligand exhibits two bonding modes (NS and ONS donor sets). In complexes **I, II, IV** and **V** (**I,** M = Cu; **II,** M = Ni; **IV,** M = Hg; **V,** M = Zn), the ligand acts as a monoanionic bidentate coordinated to the metal ion via the deprotonated enamine nitrogen and thione sulfur atoms (NS donor set) whereas in complexes **III** and **VI** (**III,** M = Mn; **VI,** M = Sn) as a monoanionic tridentate via the carbonyl oxygen, deprotonated enamine nitrogen and thione sulfur atoms (ONS donor set). Suggested structures for new complexes are shown in Fig. 3.

5. Supplementary material

Full crystallographic data (CCDC No. 213725 for ligand and CCDC No. 211558 for complex **VI**) have been deposited at the Cambridge Crystallographic Database Centre and are available on request from the Director, CCDC, 12 Union Road, Cambridge, CB2 1EZ, UK (fax: +44-1223-336033; e-mail: deposit@ccdc.cam.ac.uk or http//www.ccdc.cam.ac.uk).

Acknowledgements

Y.C. Shi thanks the National Nature Science Foundation of China (No. 20175023) and Yangzhou University (No. D0009107) for financial support of this work.

References

[1] Y.M. Temerk, A.A.M. Aly, M.M. Kamal, S.A. Ibrahim, J. Prakt. Chemie 328 (1986) 285.
[2] Y.C. Shi, Q.B. Song, X.L. Wu, Y.X. Ma, Polyhedron 13 (1994) 2101.
[3] Q.B. Song, X.L. Wu, Y.M. Liang, G.S. Huang, Y.X. Ma, Polyhedron 15 (1996) 1303.
[4] D.X. West, M.M. Salberg, G.A. Bain, A.E. Liberta, Transition Met. Chem. 22 (1997) 180.
[5] Z. Huszti, G. Szilayi, E. Kasztreiner, Biochem. Pharmacol. 32 (1983) 627.
[6] D.K. Johnson, T.B. Murphy, N.J. Rose, W.H. Goodwin, L. Pickart, Inorg. Chim. Acta 67 (1982) 259.
[7] N.K. Singh, S.K. Kushawaha, A. Srivastava, A. Sodhi, Synth. React. Inorg. Met.-Org. Chem. 32 (2002) 1743.
[8] E.I. Edwards, R. Epton, G. Marr, J. Organometal. Chem. 85 (1975) C23.
[9] M. Cais, Nature 270 (1977) 534.
[10] K.N. Zelenin, I.P. Bezhan, B.A. Brshov, A.K. Zelenin, Tetrahedron 50 (1994) 11447.
[11] W. Wang, F.L. Zeng, X. Wang, M.Y. Tan, Polyhedron 15 (1996) 1699.
[12] M.T.H. Tarafder, A. Kasbollah, K.A. Crouse, A.M. Ali, B.M. Yamin, H.-K. Fun, Polyhedron 20 (2001) 2363.
[13] C.E. Cain, T.A. Mashburn, C.R. Hauser, J. Org. Chem. 26 (1960) 1030.
[14] Y.C. Shi, H.M. Yang, W.B. Shen, C.G. Yan, X.Y. Hu, Polyhedron 22 (2003) Xref: S0277-5387(03)00608-9.
[15] G.M. Sheldrick, SMART 5.0 and SAINT 4.0 for Windows NT, Area Detector Control and Integration Software, Bruker Analytical X-ray Systems, Inc., Madison, WI, 1998.
[16] G.M. Sheldrick, SADABS Program for Empirical Absorption Correction of Area Detector Data, University of Gottingen, University of Gottingen, Germany, 1996.
[17] G.M. Sheldrick, SHLXTL 5.10 for Windows NT, Structure Determination Software, Bruker Analytical X-ray Systems, Inc., Madison, WI, 1998.
[18] Z.L. Liu, Y.Q. Tu, Synth. React. Inorg. Met.-Org. Chem. 32 (2002) 265.
[19] S. Jayasree, K.K. Aravindakshan, Polyhedron 12 (1993) 1187.
[20] E.W. Ainscough, A.M. Brodie, A.J. Dobbs, J.M. Waters, Inorg. Chim. Acta 267 (1998) 27.
[21] M. Akbar Ali, A.H. Mirza, R.J. Butcher, M.T.H. Tarafder, M.A. Ali, Inorg. Chim. Acta 320 (2001) 1.
[22] S. Shanmuga Sundara Raj, B.M. Yamin, Y.A. Yussof, M.T.H. Tarafder, H.-K. Fun, K.A. Grouse, Acta Cryst. C 56 (2000) 1236.
[23] J.D. Dunitz, L.E. Orgel, A. Rich, Acta Cryst. 9 (1956) 373.
[24] B.E. Douglas, D.H. McDaniel, J.J. Alexander, Concepts and Models of Inorganic Chemistry, Wiley, New York, 1983.
[25] L.J. Tian, B. Zhao, Q.S. Yu, Z.C. Shang, Synth. React. Inorg. Met.-Org. Chem. 32 (2002) 1177.
[26] M.D. Timken, S.R. Wilson, D.N. Hendrickson, Inorg. Chem. 24 (1985) 3450.
[27] Y.C. Shi, J. Coord. Chem., submitted.